

An extragalactic gamma-ray binary formed in supernova 2022jli

Pengfei Zhang^{1,*}, Zhongxiang Wang^{1,*}, Shunhao Ji¹

¹*Department of Astronomy, School of Physics and Astronomy, Key Laboratory of Astroparticle Physics of Yunnan Province, Yunnan University, Kunming 650091, China*

On May 5 2022, a type Ic supernova (SN) explosion SN 2022jli was discovered. This SN showed additional optical emissions, which were found to exhibit 12.4-day periodic undulations and concordant periodic velocity shifts. These key features likely indicate a compact object in a binary system was formed. A faint γ -ray source was also detected at the position of the SN and upon checking the γ -ray photons' arrival times, it was revealed that the same 12.4-day periodicity was likely present. Here we report our detailed analysis results for the γ -ray source. Not only was the γ -ray emission detectable for ~ 1.5 years since the discovery time, but a strong modulation at period 12.5 day was also clearly determined. Considering the newly formed compact object to be a neutron star or a stellar-mass black hole, the putative binary, having an orbital period of 12.5 day, is likely the first extragalactic high-energy system detected. The system may serve as a valuable example for the formation of many such binaries observed in the Milky Way and nearby galaxies.

Introduction

Stars, especially massive ones, are mostly found to be formed in binary or multi-object systems^{1,2}. It has been realized that because of the binarity, the majority of massive stars will evolve as a result of their interactions with their companions³. Depending on initial conditions such as the orbital period and the masses of a binary, it will go through different series of evolutionary processes, ending up as one of different types of products². One such typical product is the X-ray binaries (XRBs); for example, a binary consisting of $20 M_{\odot}$ plus $8 M_{\odot}$ stars with a several-day orbital period will evolve into a neutron star (NS) XRB with a high-mass supergiant companion². Nearly 500 XRBs have been found within the Milky Way^{4,5,6} and more populations of XRBs have also been identified in our local group of galaxies and beyond^{7,8,9}.

XRBs are significant X-ray sources that are powered by accretion onto compact-star primaries, either NSs or black holes (BHs), from their companions. Among those in the Milky Way, less than 10 have been further classified as gamma-ray binaries (GRBs) because the energy spectra of these binaries peak at high-energy γ -rays (energies $\gtrsim 100$ MeV)^{10,11}. In addition, XRBs with relativistic collimated jets, known as microquasars, are also able to emit γ -rays. It has been understood that when the compact star is either a pulsar or a BH with jets, significant γ -ray emissions can be produced in processes involving high-energy particles provided by either the pulsar's wind or the BH's jets, respectively¹⁰.

SN 2022jli was discovered on 5 May 2022. It was a type Ic supernova (SN) occurring in the nearby galaxy NGC 157 at a distance of 22.5 megaparsec (Mpc)¹². Its optical emission was

a double-peaked type; in the declining multiband optical light curves after the second peak, 12.4-day periodic undulations were observed, and concordant periodic velocity shifts were detected in its narrow $H\alpha$ emission. These features point to the likely formation of a compact remnant, the result of the SN explosion of a massive progenitor, in a binary system with orbital period $P_{\text{orb}} \simeq 12.4 \text{ day}^{12}$. In addition, associated γ -ray emissions were reportedly detected mainly between Sept.–Dec. 2022, and a detailed check of the arrival times of 1–3 GeV photons from the direction of SN 2022jli hinted that the same 12.4-day periodicity was present in the γ -ray emission as well.

We have conducted detailed analyses of the γ -ray data obtained with the Large Area Telescope (LAT) onboard the Fermi Gamma-ray Telescope (Fermi). We report here the result, which is that there was a clear periodic modulation in the one year since the discovery time (MJD 59704.17; hereafter set as T_0) of SN 2022jli. Combining the results reported in ref. 12, this binary is likely the first extragalactic GRB observed.

Results

Signal at period 12.54 day We analyzed the Fermi LAT data for SN 2022jli and found that the γ -ray emission was likely detectable from T_0 to Oct. 27 2023 (MJD 60244; see Methods section ‘Fermi γ -ray data and source model’), much longer than that previously reported in ref. 12. By applying a modified aperture photometry method to the data in that time period, we constructed a time series of 500 s binned counts, which were summed from probability-weighted γ -ray events in each

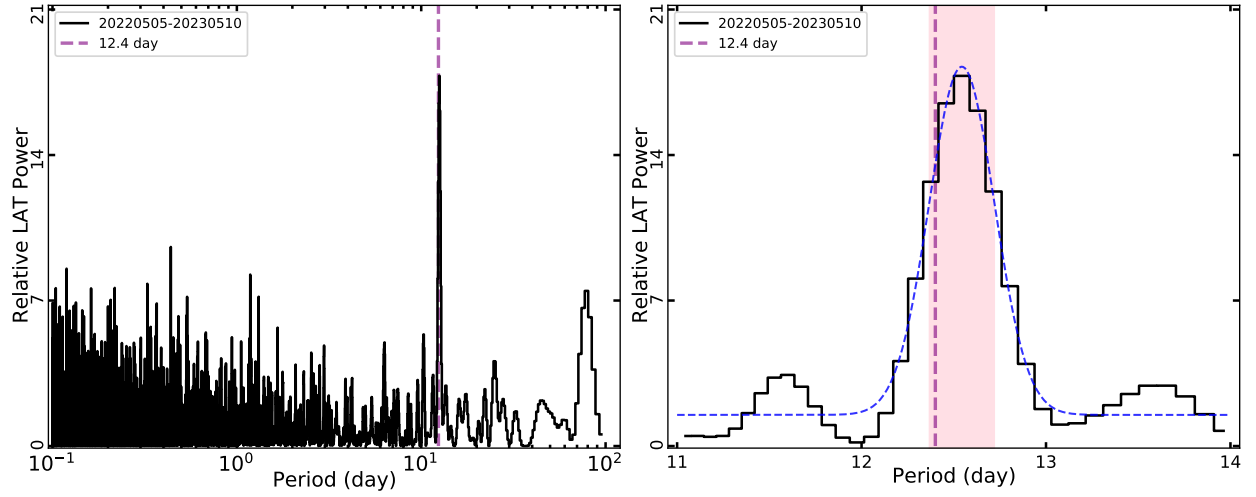


Figure 1: *Left*: LSP power spectrum of Gsrc obtained from the LAT data from May 5 2022 to May 10 2023. A periodic signal near 12.4 day is clearly visible. *Right*: LSP power spectrum of Gsrc in a frequency window of from $1/14.0$ to $1/11.0 \text{ day}^{-1}$. A Gaussian fit (blue dashed line) was used to determine the period and its uncertainty $P = 12.54 \pm 0.18 \text{ day}$ (marked by the pink region). In both panels, the 12.4-day value is marked with a purple dashed line.

time bin. The events were in the energy range of 0.1–500 GeV, selected in a 6° radius aperture with the center placed at the γ -ray counterpart (hereafter named as Gsrc) to SN 2022jli (see Methods section ‘Periodicity determination’). Applying the Lomb-Scargle Periodogram (LSP)^{13,14,15} analysis to the time series, the resulting power spectrum clearly shows a periodic signal near the reported 12.4-day period¹², which was found to have a maximum power value of 17.8 in the time period of T_0 to approximately May 10 2023 (MJD 60074; left panel of Fig. 1). By fitting the power peak with a Gaussian function (right panel of Fig. 1), we determined the period $P = 12.54 \pm 0.18$ day. This signal was estimated to be at a confidence level of 5.3σ (see Methods section ‘Periodicity determination’).

Phase-resolved properties of the γ -ray emission from SN 2022jli Using this period, which is consistent with the 12.4-day period within the uncertainty, a folded γ -ray light curve whose phase zero was set at T_0 was constructed (left panel of Fig. 2; see Methods section ‘Phase-resolved analysis’). The light curve shows that the γ -ray emission was detected only in phase 0.0–0.4, which matches the rising part of the optical undulations. Phase-resolved spectra from phase 0.0–0.4 and phase 0.2–0.3 were obtained, where the latter phase range is that of the modulation peak. The spectra were detected in an energy range of ~ 0.1 –3 GeV, described with a power law (PL) with photon indices of $\simeq 2.2$. Comparing the spectra with that obtained from the data of the whole detectable time period (i.e., from T_0 to MJD 60244), no significant spectral differences could be determined.

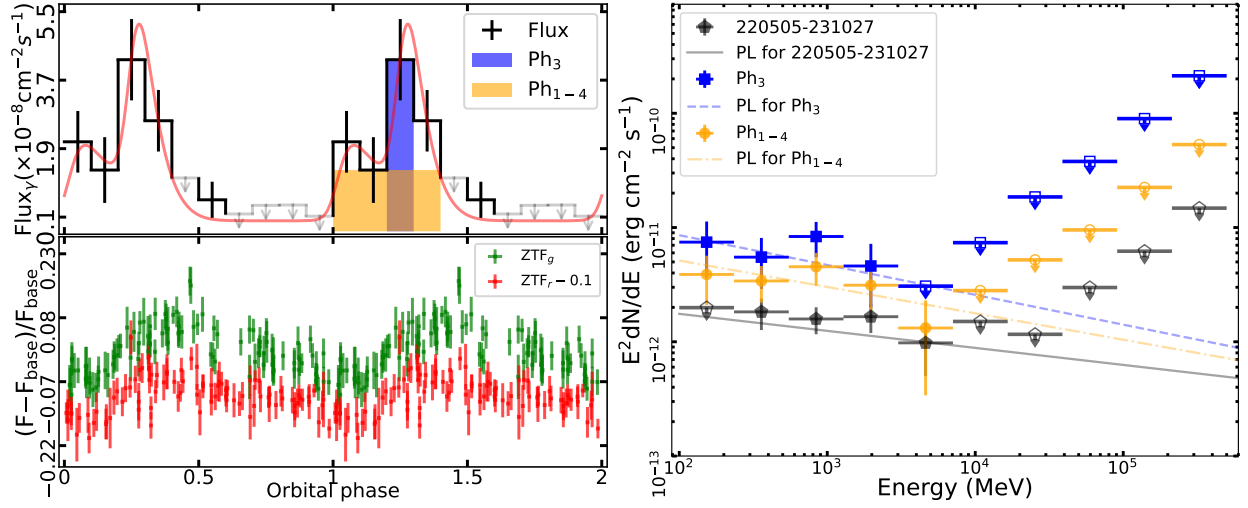


Figure 2: *Left*: folded γ -ray light curve (*top*) and ZTF optical light curves (*bottom*). A model fit, consisting of a jet plus a counter-jet with the jets' height being 1.6×10^{12} cm (see ref. 20 for details), to the γ -ray light curve is shown (red solid line). *Right*: spectra obtained from the data in Ph₃ (blue) and Ph₁₋₄ (orange), where the phase ranges are marked blue and orange respectively in the left top panel. For comparison, the spectrum from the data in the whole detectable time period (i.e., from May 5 2022 to Oct. 27 2023) is also shown. The PL fits to the spectra are respectively plotted as the blue dashed line, orange dash-dotted line, and black solid line.

Discussion

It has been extensively discussed for every aspect of SN 2022jli that this SN was likely an explosion in a binary system¹². The key features are the periodic undulations seen in optical light curves and concordant periodic velocity shifts seen in the narrow $H\alpha$ emission line. The emissions related to the second peak of the optical light curves were induced by accretion onto the compact star that was newly formed in the SN, thus revealing the orbital periodicity, and the narrow $H\alpha$ line was due to the hydrogen material contained in the accreted mass from the envelope of the companion star. While deep X-ray observations conducted at the end of the optical light curves only resulted in non-detection upper limits, the non-detection could be because of the large optical depth caused by the surrounding ejecta of the SN.

According to the orbital period distributions of Galactic XRBs, a $P_{\text{orb}} \simeq 12.5$ day system would be more likely to be a so-called high-mass XRB (HMXB)^{4,6} if the companion of the binary in SN 2022jli is a high-mass, $\sim 10 M_{\odot}$ star that will have strong mass loss either through its wind or by overfilling its Roche lobe in the subsequent evolutionary years. Indeed, in order to match the observed $H\alpha$ velocity shifts, the possible mass of the companion could be, for example, 5 or $15 M_{\odot}$ for a NS primary, or $50 M_{\odot}$ for a $10 M_{\odot}$ BH primary (see Extended Data Fig. 10 in ref. 12). When the companion components of XRBs are considered, Galactic GRBs belong to the HMXB class since their companions are $\sim 10\text{--}30 M_{\odot}$ spectral-type O/B stars^{10,11}. In this regard, SN 2022jli's binary would be the first extragalactic GRB observed.

The γ -ray emission of this putative binary was described with a PL, and its folded light curve

was highly modulated. These properties are different from those of Galactic GRBs as their γ -ray emissions are similar to that of a pulsar, often described with a PL with an exponential cutoff at several GeV energies¹⁰; it has been tentatively argued that all the GRBs have a pulsar primary. Instead, the γ -ray properties are reminiscent of those of the Galactic microquasars, namely Cygnus X-1^{16,17} and Cygnus X-3^{18,19}. These two XRBs were observed to have γ -ray emissions during their hard state when jets were present; the emissions were well fitted with a PL, and those of Cygnus X-3 were highly modulated on its orbital period.

The γ -ray emissions of Cygnus X-3 are well explained with a model that considers anisotropic Compton scattering of blackbody photons from the companion by the relativistic electrons of its jets^{19,20}. We tested to use this model to fit the folded light curve, where we adopted the BH binary system that can provide a match to the velocity shifts (i.e., $10 M_{\odot}$ BH, $50 M_{\odot}$ companion, orbital eccentricity $e = 0.8$, and inclination angle of the binary $i = 90^{\circ}$; ref. 12). The radius ($\sim 8 \times 10^{11}$ cm) and effective temperature ($\sim 5 \times 10^4$ K) of the companion were estimated from the relations given in ref. 21. Because there are a few parameters in the model (in which a jet plus a counter-jet are included; see details in ref. 20) and limited information is known for the putative binary, we fixed the bulk velocity of the jets at $0.1c$ (where c is the light speed) and the polar angle of the jets at 60° (note that 0° is when the jets are perpendicular to the orbital plane), and found that the jets with a height of $\sim 1.6 \times 10^{12}$ cm can provide acceptable fits to the folded light curve (left panel of Fig. 2). It is interesting to note that the BH binary system we adopted has a separation distance of 1.2×10^{12} cm at periastron, which is comparable to the jets' size. This is similar to that found in the microquasars^{10,20}.

The detection of the γ -ray emission highly modulated on the optical-undulation period greatly strengthens the likelihood of a compact-star binary forming in SN 2022jli. At a distance of 22.5 Mpc, if the compact star is a NS or a stellar-mass BH, it would have experienced super-Eddington accretion in order to power the observed optical undulation emission¹². The apparent γ -ray luminosity of this putative binary (Table 1) was also >1000 times the Eddington limit (for a stellar-mass compact star), potentially making it an ultraluminous γ -ray source, in parallel to the ultraluminous X-ray sources detected in the X-ray sky²².

Methods

Fermi γ -ray data and source model The Large Area Telescope (LAT) onboard the Fermi Gamma-ray Space Telescope (Fermi) has been scanning the entire sky since Aug. 2008. We selected LAT’s Pass 8 Front+Back events (evclass = 128, evtype = 3) in the 0.1–500 GeV energy range from Aug. 4 2008 to Jul. 7 2025 (MJD 54682.687–60863.123). A $20^\circ \times 20^\circ$ region of interest (RoI) was set with the center placed at the position of the new γ -ray source¹² (i.e., Gsrc), R.A. = $8^\circ.620$, Decl. = $-8^\circ.425$ (J2000.0). To minimize γ -ray contamination from the Earth’s limb, we excluded events with zenith angle $> 90^\circ$. High-quality events within good time intervals were selected by applying the filter expression “DATA_QUAL >0 && LAT_CONFIG==1.” The “P8R3_SOURCE_V3” instrument response function and Fermitools 2.2.0 were used in our analyses.

A source model was built based on the Fourth Fermi Gamma-ray LAT (4FGL) catalog Data Release 4 (4FGL-DR4)²³, with Gsrc added in as a point source, by running the Python script make4FGLxml.py. A power-law (PL) spectral form, $dN/dE = N_0(E/E_0)^{-\Gamma}$, where Γ is the PL

index, was used for the emission of Gsrc. The Galactic and extragalactic isotropic components, files `gll_iem_v07.fits` and `iso_P8R3_SOURCE_V2_v1.txt` respectively, were also included in the source model. In our following analyses, the normalizations of these two background components were always set as free parameters.

The data in our analyses were from ~ 17 years of LAT observations, longer than the 14 years of the data used to build 4FGL-DR4. We thus updated the parameters in the source model by performing binned maximum likelihood analysis. In this analysis, flux normalizations and spectral parameters of sources within 5° of Gsrc were set free, flux normalizations of sources within 5° – 10° and variable sources $>10^\circ$ of Gsrc were also set free, and all other parameters were fixed at values given in 4FGL-DR4. From this analysis, we obtained a TS value of 22.8 for Gsrc; the best-fit parameters were $\Gamma = 2.51 \pm 0.20$ and photon flux $F_{\text{ph}} = 2.8 \pm 1.3 \times 10^{-9}$ photons $\text{cm}^{-2} \text{s}^{-1}$ in 0.1–500 GeV. These values are also provided in Table 1.

We then constructed a 0.1–500.0 GeV light curve for Gsrc by binning the LAT data into 90-day intervals and performing likelihood analysis to the binned data. To check possible details of the light curve, we also constructed a smooth light curve by shifting each 90-day time bin 5 day forward. The light curves (left panel of Fig. 3) show that prior to T_0 (i.e., MJD 59704.17), no γ -ray emission was detected from SN 2022jli, but after a flux peak before the end of 2022, Gsrc was detectable possibly up until Oct. 27 2023 (MJD 60244). We performed likelihood analysis to the data from T_0 to MJD 60244, and obtained a TS value of 78.1; the other measurements are provided in Table 1. In addition, we also tested the analysis for the data from T_0 to May 10 2023 (MJD 60074; see section ‘Periodicity determination’ below) and from MJD 60074 to 60244, and

obtained TS values of 50.3 and 21.2, respectively. These results confirm the light-curve results that the γ -ray emission was detectable before Oct. 27 2023.

By running the tool `gtfindsrc` to >1 GeV data in the ~ 1.5 -year time period from T_0 to MJD 60244, we obtained the position of Gsrc: R.A. = $8^\circ.57$, Decl. = $-8^\circ.46$ (J2000.0), with a 3σ uncertainty of $0^\circ.16$. SN 2022jli is within this uncertainty region. We updated our source model by using this position for Gsrc. We noted that the analyses were not sensitive to the two positions, as the light curves and best-fit results from the binned likelihood analysis were nearly identical.

Periodicity determination We constructed an aperture light curve using the source model file obtained above to search and determine the periodicity, where a modified aperture photometry (AP) method was employed. First, since Gsrc was a faint γ -ray source, events within a 6° radius¹ aperture in 0.1–500 GeV were selected. To mitigate γ -ray contamination from the Sun or the Moon, we excluded the data from time periods when Gsrc was within 5° of the Sun or the Moon, as determined from `gtmktime`. Second, time bins of 500 s each were set, and the LAT exposures of the time bins were taken into account, where the exposures were obtained from the tool `gtexposure`. We then calculated the probabilities of the events originating from Gsrc using `gtsrcprob`, and summed them within each time bin^{24,25,26}. The probability values, rather than the raw event counts, were taken as the counts of the time bins. Third, barycentric corrections to the arrival times of the time bins were applied by using the tool `gtbary`, which considered the motion of both the Earth and the Fermi satellite relative to the Solar system’s barycenter.

¹68% containment angle of the LAT at 0.1 GeV; https://www.slac.stanford.edu/exp/glast/groups/canda/lat_Performance.htm

In performing the timing analysis, we utilized the Lomb-Scargle Periodogram (LSP)^{13,14,15} to compute the power spectrum from the AP light curve. A periodic signal near the 12.4-day optical undulation period was easily found from the power spectrum (e.g., the left panel of Fig. 1). However, given the period was known, we instead conducted periodicity search analysis in an 11.0- to 14.0-day window. A periodic signal at ~ 12.5 day was found from the AP light curve spanning from T_0 to MJD 60244. Because temporal changes in γ -ray orbital signals were seen in some binary systems^{27,28,29}, we examined the variations of this 12.5-day signal by using AP light curves of different lengths, all starting from T_0 with a 30-day time step. The results are shown in the right panel of Fig. 3. The signal peak reached a maximum power value of ~ 17.8 on May 10 2023 (MJD 60074). By fitting this power peak with a Gaussian function, the period was determined to be 12.54 ± 0.18 day, where the uncertainty was the full width at half maximum of the Gaussian fit (see the right panel of Fig. 1). We note that the period is consistent with the optical one within the uncertainty.

In calculating the power spectrum, a frequency range was set from $f_{\min} = 1/14.0 \text{ day}^{-1}$ to $f_{\max} = 1/11.0 \text{ day}^{-1}$, with a frequency resolution of $\delta f = 1/T_{\text{obs}}$, where T_{obs} is the time duration of the AP light curve (i.e., $\delta f = 1/370 \text{ day}^{-1}$). The number N of independent frequencies was $N = (f_{\max} - f_{\min})/\delta f \simeq 7$, which could be taken as the trial factor. Additionally, an oversampling factor of 5 was adopted^{26,29,30}. Assuming Gaussian white noise, we estimated the probability p_{lsp} of detecting a periodic signal with a power level of 17.8 by chance, $p_{\text{lsp}} \sim 1.82 \times 10^{-8}$. Accounting for the trial factor N , the corresponding false alarm probability (FAP) was $\text{FAP} = 1 - (1 - p_{\text{lsp}})^N \simeq N \times p_{\text{lsp}} = 1.27 \times 10^{-7}$, which corresponds to a confidence level of $\sim 5.3\sigma$. We note that because

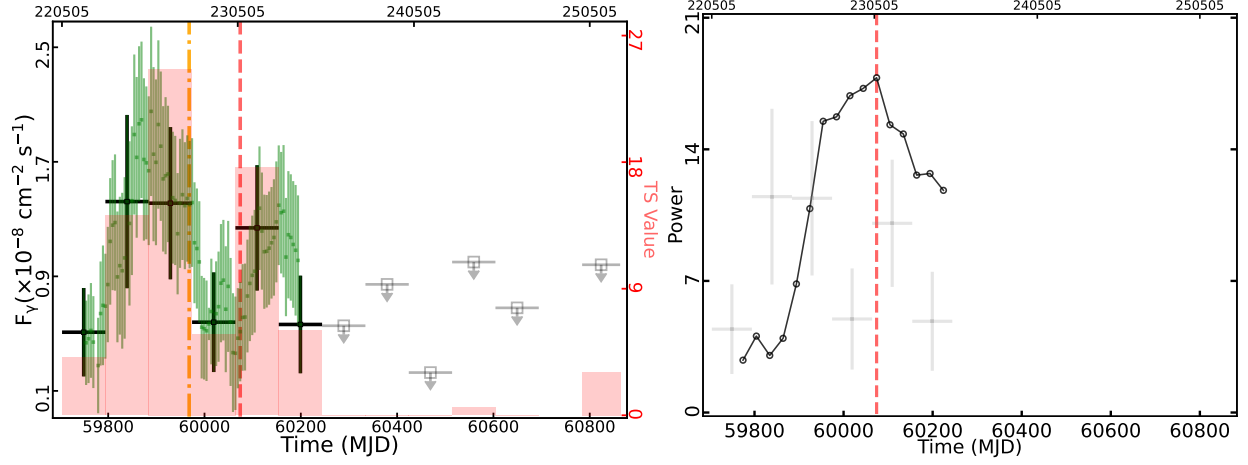


Figure 3: *Left*: 90-day binned light curve (black data points) of Gsrc in 0.1–500 GeV from T_0 to Jul. 7 2025. The TS values of the data points are indicated by the red histogram. After \sim MJD 60244, the source was undetected. A smooth light curve (green data points), with each 90-day time bin shifted by 5 day forward, is also shown for comparison. The end of the optical light curves of SN 2022jli in ref. 12 is marked by the orange dash-dotted line and the date of May 10 2023 (MJD 60074) is marked by the red dashed line. *Right*: power peak values of the \sim 12.5-day signal, obtained from LSP analysis of AP light curves of different lengths (all starting from T_0 with a 30-day time step). The maximum value is 17.8 (marked by the red dashed line), when the AP light curve is from T_0 to May 10 2023.

the period can be considered known, we could set analysis with $N = 1$, which would increase the confidence level to 5.6σ .

Phase-resolved analysis Based on the periodicity we obtained above, we divided the LAT data in the time range of T_0 to MJD 60074 into 10 periodic phase intervals, with phase zero set at T_0 . A folded light curve in 0.1–500 GeV was obtained by performing likelihood analysis to the data in each phase interval. In this analysis, the flux normalizations of sources within 5° of Gsrc were allowed to vary, while all other parameters were fixed at the values in our source model above (from the data of T_0 to MJD 60244). For the obtained flux data points, those with $TS \geq 4$ were kept; otherwise, the 95% flux upper limits were derived and used (left panel of Fig. 2). The emission of Gsrc was highly variable, as it was detected in the phase range of 0.0–0.4 (defined as Ph_{1-4}) and the flux peak was at phase 0.2–0.3 (defined as Ph_3). To examine the emission properties, we performed likelihood analysis to the data in Ph_{1-4} and Ph_3 , where the parameters were set as the above. The results are provided in Table 1.

It is interesting to compare the γ -ray modulation with the optical undulation. We used the g and r band data from the Zwicky Transient Facility (ZTF) and followed the analysis method in ref. 12 but set the period at 12.54 day. The obtained undulation profiles (left panel of Fig. 2) are very similar to those reported in ref. 12.

We also obtained the spectra for Gsrc in Ph_{1-4} and Ph_3 by dividing the energy range of 0.1–500 GeV into 10 bins equally spaced in logarithmic energy and performing likelihood analysis to the data in each bin. The same parameter setup as the above was applied. For the obtained

data points, those with $TS \geq 4$ were kept; otherwise, the 95% upper limits were derived and used instead. For comparison, we also obtained the spectrum in the T_0 to MJD 60244 time period (i.e., the total data for Gsrc). The same analysis was performed. No significant differences among the spectra could be determined (see the right panel of Fig. 2 and Table 1).

Data Availability

The data results that support the findings of this study are available from the corresponding authors upon reasonable request.

1. Moe, M. & Di Stefano, R. Mind Your Ps and Qs: The Interrelation between Period (P) and Mass-ratio (Q) Distributions of Binary Stars. *Astrophys. J. Suppl. S.* **230**, 15 (2017). 1606.05347.
2. Tauris, T. M. & van den Heuvel, E. P. J. *Physics of Binary Star Evolution. From Stars to X-ray Binaries and Gravitational Wave Sources* (2023).
3. Sana, H. *et al.* Binary Interaction Dominates the Evolution of Massive Stars. *Science* **337**, 444 (2012). 1207.6397.
4. Fortin, F., García, F., Simaz Bunzel, A. & Chaty, S. A catalogue of high-mass X-ray binaries in the Galaxy: from the INTEGRAL to the Gaia era. *Astron. Astrophys.* **671**, A149 (2023). 2302.02656.

5. Neumann, M., Avakyan, A., Doroshenko, V. & Santangelo, A. XRBcats: Galactic High Mass X-ray Binary Catalogue. *Astron. Astrophys.* **677**, A134 (2023). 2303.16137.
6. Fortin, F., Kalsi, A., García, F., Simaz-Bunzel, A. & Chaty, S. A catalogue of low-mass X-ray binaries in the Galaxy: From the INTEGRAL to the Gaia era. *Astron. Astrophys.* **684**, A124 (2024). 2401.11931.
7. Liu, Q. Z., van Paradijs, J. & van den Heuvel, E. P. J. High-mass X-ray binaries in the Magellanic Clouds. *Astron. Astrophys.* **442**, 1135–1138 (2005).
8. Liu, Q. Z., van Paradijs, J. & van den Heuvel, E. P. J. A catalogue of low-mass X-ray binaries in the Galaxy, LMC, and SMC (Fourth edition). *Astron. Astrophys.* **469**, 807–810 (2007). 0707.0544.
9. Gilfanov, M., Fabbiano, G., Lehmer, B. & Zezas, A. X-Ray Binaries in External Galaxies. In Bambi, C. & Santangelo, A. (eds.) *Handbook of X-ray and Gamma-ray Astrophysics*, 105 (2022).
10. Dubus, G. Gamma-ray binaries and related systems. *Astron. Astrophys. Rev.* **21**, 64 (2013). 1307.7083.
11. Chernyakova, M. & Malyshev, D. Gamma-ray binaries. In *Multifrequency Behaviour of High Energy Cosmic Sources - XIII. 3-8 June 2019. Palermo*, 45 (2020). 2006.03615.
12. Chen, P. *et al.* A 12.4-day periodicity in a close binary system after a supernova. *Nature* **625**, 253–258 (2024). 2310.07784.

13. Lomb, N. R. Least-Squares Frequency Analysis of Unequally Spaced Data. *Astrophys. Space Science* **39**, 447–462 (1976).
14. Scargle, J. D. Studies in astronomical time series analysis. II. Statistical aspects of spectral analysis of unevenly spaced data. *Astrophys. J.* **263**, 835–853 (1982).
15. Zechmeister, M. & Kürster, M. The generalised Lomb-Scargle periodogram. A new formalism for the floating-mean and Keplerian periodograms. *Astron. Astrophys.* **496**, 577–584 (2009). 0901.2573.
16. Malyshev, D., Zdziarski, A. A. & Chernyakova, M. High-energy gamma-ray emission from Cyg X-1 measured by Fermi and its theoretical implications. *Mon. Not. R. Astron. Soc.* **434**, 2380–2389 (2013). 1305.5920.
17. Zdziarski, A. A., Malyshev, D., Chernyakova, M. & Pooley, G. G. High-energy gamma-rays from Cyg X-1. *Mon. Not. R. Astron. Soc.* **471**, 3657–3667 (2017). 1607.05059.
18. Fermi LAT Collaboration *et al.* Modulated High-Energy Gamma-Ray Emission from the Microquasar Cygnus X-3. *Science* **326**, 1512 (2009).
19. Zdziarski, A. A. *et al.* A comprehensive study of high-energy gamma-ray and radio emission from Cyg X-3. *Mon. Not. R. Astron. Soc.* **479**, 4399–4415 (2018). 1804.07460.
20. Dubus, G., Cerutti, B. & Henri, G. The relativistic jet of Cygnus X-3 in gamma-rays. *Mon. Not. R. Astron. Soc.* **404**, L55–L59 (2010). 1002.3888.

21. Eker, Z. *et al.* Main-Sequence Effective Temperatures from a Revised Mass-Luminosity Relation Based on Accurate Properties. *Astron. J.* **149**, 131 (2015). 1501.06585.
22. Pinto, C. & Walton, D. J. Ultra-luminous X-ray sources: extreme accretion and feedback. *arXiv e-prints* arXiv:2302.00006 (2023). 2302.00006.
23. Ballet, J., Bruel, P., Burnett, T. H., Lott, B. & The Fermi-LAT collaboration. Fermi Large Area Telescope Fourth Source Catalog Data Release 4 (4FGL-DR4). *arXiv e-prints* arXiv:2307.12546 (2023). 2307.12546.
24. Kerr, M. Improving Sensitivity to Weak Pulsations with Photon Probability Weighting. *Astrophys. J.* **732**, 38 (2011). 1103.2128.
25. Fermi LAT Collaboration *et al.* Periodic Emission from the Gamma-Ray Binary 1FGL J1018.6-5856. *Science* **335**, 189 (2012). 1202.3164.
26. Corbet, R. H. D. *et al.* Discovery of the Galactic High-mass Gamma-Ray Binary 4FGL J1405.1-6119. *Astrophys. J.* **884**, 93 (2019). 1908.10764.
27. Ng, C. W., Takata, J., Strader, J., Li, K. L. & Cheng, K. S. Evidence on the Orbital Modulated Gamma-Ray Emissions from the Redback Candidate 3FGL J2039.6-5618. *Astrophys. J.* **867**, 90 (2018).
28. Clark, C. J. *et al.* Einstein@Home discovery of the gamma-ray millisecond pulsar PSR J2039-5617 confirms its predicted redback nature. *Mon. Not. R. Astron. Soc.* **502**, 915–934 (2021). 2007.14849.

29. Corbet, R. H. D. *et al.* Gamma-Ray Eclipses and Orbital Modulation Transitions in the Candidate Redback 4FGL J1702.7-5655. *Astrophys. J.* **935**, 2 (2022). 2203.05652.
30. Corbet, R. H. D. *et al.* A Luminous Gamma-ray Binary in the Large Magellanic Cloud. *Astrophys. J.* **829**, 105 (2016). 1608.06647.

Acknowledgements This work is supported in part by the National Natural Science Foundation of China under grant Nos. 12233006, 12163006, and 12273033, and the joint foundation of Department of Science and Technology of Yunnan Province and Yunnan University (grant No. 202201BF070001-020). P.Z. acknowledges the support by the Xingdian Talent Support Plan–Youth Project.

Contributions P.Z. led the analysis and made the initial discovery. Z.W. provided explanations and wrote most of the text. S.J. aided the explanations. All authors discussed the results and manuscript.

Competing Interests The authors declare that they have no competing financial interests.

Correspondence Correspondence and requests for materials should be addressed to P.Z. (email: zhanngpengfei@ynu.edu.cn) and Z.W. (email: wangzx20@ynu.edu.cn).

Table 1: Results of likelihood analyses

Time range	TS	Γ	F_{ph}	F_{en}	L_{γ}
20080804–20250707	22.6	2.50 ± 0.20	2.68 ± 0.80	1.26 ± 0.41	0.76 ± 0.25
20220505–20231027	78.1	2.15 ± 0.12	9.5 ± 2.4	8.5 ± 1.8	5.1 ± 1.1
20230510–20231027	21.2	2.10 ± 0.20	9.3 ± 3.8	9.3 ± 3.8	5.7 ± 2.3
20220505–20230510	50.3	2.25 ± 0.16	10.9 ± 3.3	7.7 ± 1.7	4.6 ± 1.0
Phase	Phase-resolved analysis				
Ph _{1–4}	81.5	2.23 ± 0.13	26.1 ± 6.0	19.1 ± 4.1	11.6 ± 2.5
Ph ₃	34.5	2.26 ± 0.19	42 ± 14	29.3 ± 7.4	17.7 ± 4.5

Notes. The integrated photon flux (F_{ph}) is given in units of 10^{-9} photons $\text{cm}^{-2} \text{s}^{-1}$, the integrated energy flux (F_{en}) in units of 10^{-12} erg $\text{cm}^{-2} \text{s}^{-1}$, and the γ -ray luminosity (L_{γ}) at a distance of 22.5 Mpc in units of 10^{41} erg s^{-1} .